

Impurity Behavior in High Performance ADITYA Tokamak Plasmas^{*)}

Malay B. CHOWDHURI¹⁾, Ranjana MANCHANDA¹⁾, Joydeep GHOSH^{1,2)}, Nandini YADAVA³⁾, Sharvil PATEL⁴⁾, Nilam RAMAIYA¹⁾, Anand K. SRIVASTAVA⁵⁾, Kumudni TAHILIANI¹⁾, Meduri V. GOPALAKRISHNA¹⁾, Umesh C. NAGORA¹⁾, Praveen K. ATREY¹⁾, Surya K. PATHAK^{1,2)}, Shishir PUROHIT¹⁾, Joisa SHANKARA¹⁾, Kumarpalsinh A. JADEJA¹⁾, Rakesh L. TANNA¹⁾, Chet N. GUPTA¹⁾, Prabal K. CHATTOPADHYAY^{1,2)} and ADITYA Team¹⁾

¹⁾Institute for Plasma Research, Bhat, Gandhinagar 382 428, India

²⁾Homi Bhabha National Institute, Training School Complex, Anushaktinagar, Mumbai 400 094, India

³⁾Institute of Science, Nirma University, Ahmedabad 382 481, Gujarat, India

⁴⁾Pandit Deendayal Energy University, Raisan, Gandhinagar, 382 007, Gujarat, India

⁵⁾Birla Institute of Technology-Mesra, Jaipur Campus, Jaipur 302 017, India

(Received 31 December 2021 / Accepted 3 February 2022)

Impurity behavior has been studied for the high performance Ohmically heated ADITYA tokamak plasmas operated with higher toroidal magnetic field and multiple gas puffs. The neutral hydrogen and impurity emissions in the visible range were monitored by photo multiplier tube (PMT) based system in which interference filter used for wavelength selection. The VUV spectral line emissions from impurities, such as C^{4+} , O^{5+} and Fe^{14+} , were also recorded by a VUV survey spectrometer operated in the 10 - 180 nm. It has been found that H_{α} , O^{1+} , and C^{2+} emissions normalized with electron density (n_e), and visible continuum normalized with n_e^2 show a gradual decrease with increase in density indicating lower impurity concentration in these discharges. The VUV emission also shows the similar trend with increasing n_e . Indeed, the impurity transport study using iron emissions confirms that the iron concentration reduces with increasing n_e . This is also corroborated by the observed reduction in plasma effective charge, Z_{eff} and radiation power loss with the increase in n_e . These results clearly indicate that the improved confinement for ADITYA plasma are correlated with reduction of impurities concentration in those discharges.

© 2022 The Japan Society of Plasma Science and Nuclear Fusion Research

Keywords: impurity, visible, VUV, spectroscopy, plasma, ADITYA tokamak

DOI: 10.1585/pfr.17.2402011

1. Introduction

Higher plasma confinement and steady state operation of plasma are the primary goals to achieve sustainable fusion in the magnetically confined plasma devices. In these aspects, impurity plays a major role as it effects the plasma due to energy loss via impurity radiation. Radiated power increases remarkably with the increasing plasma density, not only due to enhancement of line radiation, but also due to increase of the bremsstrahlung radiation [1]. So, to achieve better plasma performance impurity accumulation has to be kept in control. This impurity accumulation is further enhanced in the auxiliary heated plasma. In addition to that, fuel dilution happens due to the presence of impurities in the plasma core, which effect the fusion reaction in the fusion grade plasma. The impurity mainly enters into the plasma due to the interaction of plasma particle with various plasma facing components and vacuum

vessel wall. These interaction processes are mainly reflection, desorption and sputtering. In this respect, reduction of various impurity generation processes via different techniques, such as glow and pulse discharge cleaning [2] and coating of the first wall with silicon, boron and/or lithium [3] have been investigated in details. Not only that, various control mechanisms, such as use of stochastic magnetic field structure at the plasma edge [4], and auxiliary heating, e.g., electron cyclotron heating (ECH) and ion cyclotron resonance heating (ICRH) [5] are being explored to avoid impurity accumulation in the plasma core. In many high temperature plasma devices, including the large helical device (LHD), impurity screening has been observed in the presence of ergodic layer inside the edge and scrape of layer (SoL) plasma [4]. However, to explore the mechanism behind impurity control and the physics associated with it, the detailed understanding of impurity behaviour inside the plasma is important and is studied for various types of configurations, like plasma with limiter and divertor, and plasma operations in the detached H-mode, im-

author's e-mail: malay@ipr.res.in

^{*)} This article is based on the presentation at the 30th International Toki Conference on Plasma and Fusion Research (ITC30).

proved Ohmic confinement (IOC) and radiative improved (RI) modes [6–10].

In this work, the impurity behaviour has been studied for the high performance Ohmically heated ADITYA tokamak [11] plasmas having relatively higher plasma current and electron density [12]. These discharges were operated with higher toroidal magnetic fields and thereby it sustained higher plasma current and higher densities were achieved using multiple gas puffs. High energy confinement times were observed in these discharges. Impurity behaviour in the plasma edge has been analysed using the spectral emissions measured by visible spectroscopic diagnostics installed on the tokamak. Similarly, core impurity behaviour has been investigated by monitoring vacuum ultraviolet (VUV) spectral lines emissions using a VUV survey spectroscopic system [13]. It has been found through the study that the high discharge performances are interlinked with reduced impurity content in the plasma. The details on ADITYA tokamak and various diagnostics used for the study have been described in section II. The results have been presented and discussed in section III and the paper is summarized in the final section.

2. ADITYA Tokamak and Description of Relevant Diagnostics

ADITYA tokamak [11] is a medium size tokamak with major radius (R) = 75 cm and minor radius (a) = 25 cm. It is having a poloidal ring limiter at a toroidal location and operated with toroidal magnetic field, $B_T = 0.75$ to 1.26 T. The vacuum vessel is made of stainless steel and the limiter is made of graphite. In addition to oxygen, carbon and iron present in the plasma as the impurities. In these discharges, B_T was higher than normally used 0.75 T. The plasma current was in the range of 100 to 180 kA and duration was 100 - 200 ms depending on the experimental scenario. The plasma electron temperature, T_e was ~ 350 to 800 eV and central line averaged electron density, n_e was $1 - 3 \times 10^{19} \text{ m}^{-3}$. Radial profile of electron density is measured with 7 channels microwave interferometer diagnostic spanning over whole plasma diameter [14]. The soft X-ray emission is monitored using silicon barrier diode (SBD, ORTEC make) detector and the electron temperature is measured using soft X-ray emissions by foil absorption technique. Total radiated power, P_{rad} is measured using the AXUV bolometer [15].

Photo-multiplier tube (PMT) based visible spectroscopy system has been used to monitor temporal evolution of H_α and line emissions of carbon and oxygen impurities in the visible wavelength range. The light has been collected using a collimating beam probe based on plano-convex lens having focal length of 14 mm and diameter of 9 mm. Optical fiber having core diameter of 1 mm and numerical aperture (NA) of 0.22 has been used to transport the light from radial port 2 of the tokamak. The lines of sight (LoSs) of these optical set-ups are terminated on the

inboard wall of tokamak and the viewing chord diameter is around 2.5 cm at the plasma mid-plane. The wavelengths have been selected using interference filters having diameter 5 cm and bandwidth of 1 nm. These wavelengths are 656.3, 441.6, and 464.7 nm for H_α and line emissions from O^{1+} , and C^{2+} impurities ions, respectively. The dispersed light is detected by the PMTs (part no. R374, Hamamatsu Photonics, Japan). The visible continuum around 523.4 nm wavelength has been monitored using a similar PMT based system to estimate the ADITYA plasma Z_{eff} . However, the plasma is here viewed from the top port of machine and the LoS is terminated on a view port placed on the bottom port [16]. For all the systems, data have been acquired at every 10 μs using ADITYA main data acquisition (DAQ) and stored in the data server. These systems are calibrated to obtain the absolute flux for the quantitative analysis using an absolutely calibrated integrated sphere.

A toroidal grating-based VUV survey spectroscopic system [17] has been used to monitor the impurities emission and its behaviour in the VUV range. This system was vacuum coupled to ADITYA tokamak at radial port 17 viewing the plasma along a LoS passing through the plasma center and was operated with a vacuum $\sim 1 \times 10^{-7}$ mbar. The spectrometer (model no TG-320, Jovin Yvon, France) covers three wavelength regions with different spectral resolution using three different gratings, which can be selected with the help of manually operated ultra-high vacuum (UHV) compatible linear motion feed through. In this system, 290 g/mm grating provides coverage of 15 to 170 nm with a resolution 0.68 nm and 450 g/mm grating gives a coverage 10 to 110 nm with a moderate resolution of 0.47 nm. The 2105 g/mm grating provides the best resolution of 0.18 nm but total wavelength coverage is restricted to 9.5 to 32 nm. This high groove density grating is useful to monitor the spectral lines from medium Z impurities, such as Ne, Ar and Fe, for studying impurity behaviour in the core plasma region. It can be also used to monitor the closely spaced spectral lines having $\Delta n \geq 1$ from low Z impurities, such as C and O. The VUV spectroscopic system is equipped with multi-channel plate (MCP, Burle Make) plus charge coupled device (CCD, Princeton Instrument make) detector. It has the read out time of 2.76 ms enabling us to record the spectrum at every 10 ms. Then, this is useful to study the temporal evolution of VUV emission lines during plasma discharge. This system operated with 450 g/mm grating has been utilized to observe the line emissions from higher ionized charge states of impurities, such as C^{4+} , O^{5+} , Fe^{14+} and Fe^{15+} ions to do this study. The absolute intensity calibration of the VUV survey spectroscopic system has been carried out using the combination of conventional branching ratio technique and collisional-radiative modelling technique [17], in which the intensities of VUV spectral lines of oxygen ions have been estimated and the required densities of different ionization states of oxygen have been obtained through the measurement of the spectral line emission of

O^{4+} at 650.02 nm in the visible region.

3. Results and Discussions

For the analysed discharges, the ADITYA tokamak's operation was carried out with increased toroidal magnetic field to sustain higher plasma current. In order to achieve higher electron densities, multiple gas puffs were introduced into the edge plasma using an indigenously developed automatic pulse gas feed system using piezoelectric valve. Not only that, precise plasma position control and lithium wall conditioning were done to improve the reproducibility of discharges [18]. A typical plasma discharge having shot no. 28821 has been shown in Fig. 1 containing the traces of plasma current (I_p), loop voltage (V_{loop}), line averaged electron density (n_e) and H_α emission and radiative power (P_{rad}) signals. The maximum value of plasma current, I_p was 122 kA in this discharge. The line averaged electron density, n_e was $\sim 1.5 \times 10^{19} \text{ m}^{-3}$ as shown in Fig. 1 (b). The electron temperature, T_e was $\sim 500 \text{ eV}$ until 80 ms and then decreased to $\sim 250 \text{ eV}$ when multiple gas puffs were introduced into the edge plasma and plasma current has started falling gradually after 80 ms. As shown in Fig. 1 (c), the modulations in H_α and P_{rad} signals from 80 to 140 ms arise due to the multiple numbers of gas puffing. The pulse duration of these puffs is $\sim 1 \text{ ms}$ and pe-

riod is $\sim 8 \text{ ms}$. One can also see that electron density has started increasing after the gas puff. The temporal evolution of O^{1+} , C^{2+} and visible continuum signals are shown in Fig. 2. The first and last peaks in all these signals are due to the ionization of impurities entered into the plasma during the breakdown and recombination of impurities ions during the plasma termination phases, respectively. The effect of gas puff is also visible in these signals. The plasma parameters at the time of plasma current flat top have been analysed to find their characteristics. The plasma electron temperature, T_e and the error in T_e has been plotted with respect to electron density in the Fig. 3. It is seen that T_e increases with n_e and its maximum value is $\sim 800 \text{ eV}$ for the analysed discharges. The energy confinement time, τ_E has been estimated for these discharges to understand the confinement property using the equation,

$$\tau_E = \frac{\frac{3}{2} \langle n_i T_i + n_e T_e \rangle V_p}{I_p V_1 - P_{rad}}, \quad (1)$$

where I_p is the plasma current, V_1 is the loop voltage, V_p is the plasma volume, and P_{rad} is the total radiated power. For its estimation, the temperature and density profiles have been assumed parabolic using experimentally measured central and edge values of those as the single chord measurements were available for most of the anal-

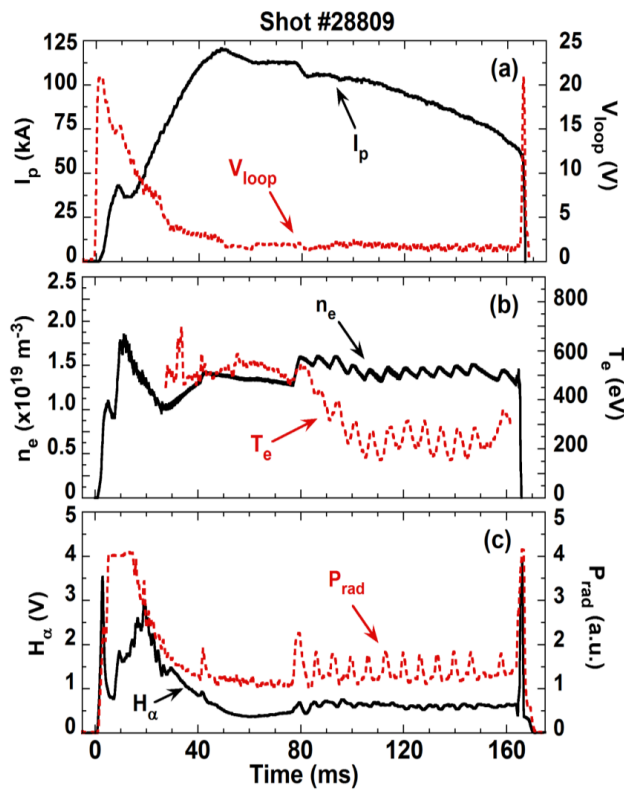


Fig. 1 Temporal evolution of (a) plasma current (I_p) and loop voltage (V_{loop}) and (b) line averaged electron density (n_e) and electron temperature (T_e) and H_α emission and radiative power (P_{rad}) for a typical ADITYA tokamak plasma.

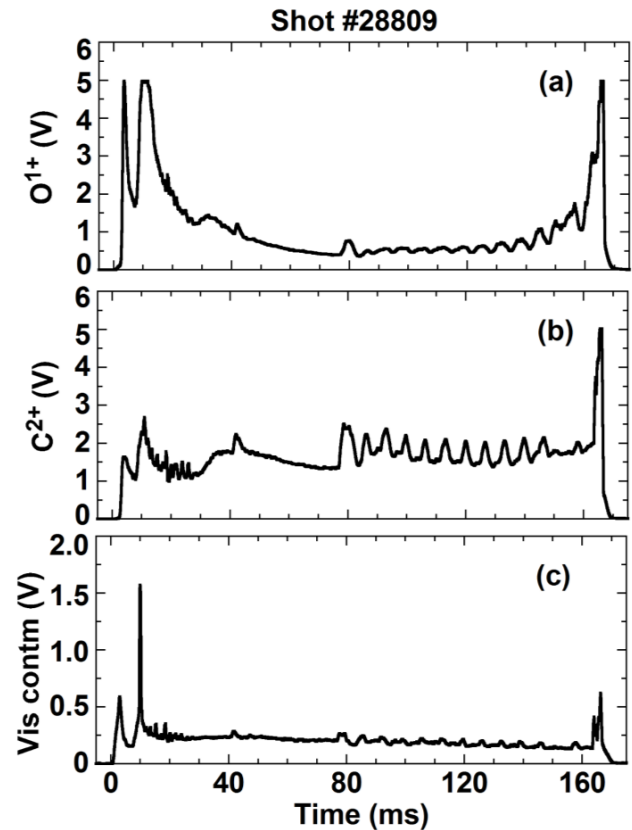


Fig. 2 Temporal evolution of spectral lines of (a) O^{1+} at 441.6 nm and (b) C^{2+} at 464.7 nm and (c) visible continuum for a typical plasma of ADITYA tokamak.

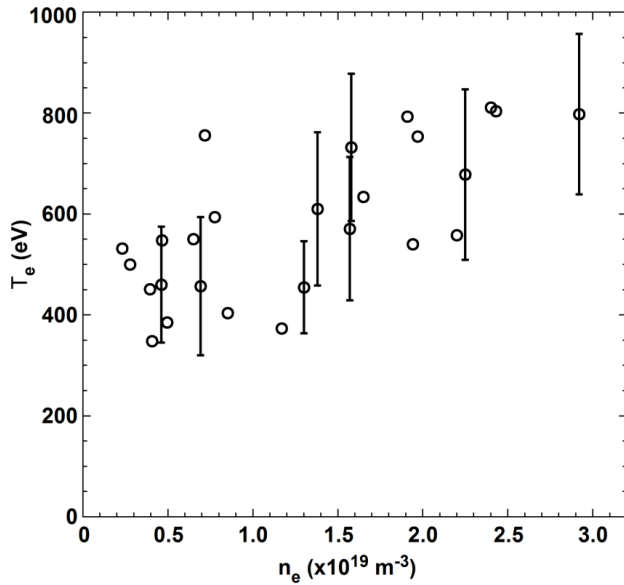


Fig. 3 Plasma electron temperature, T_e vs. electron density, n_e for the analyzed discharges.

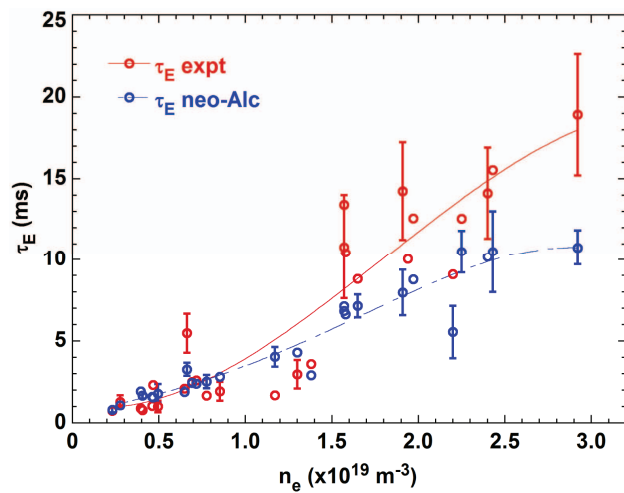


Fig. 4 Energy confinement time, τ_E plotted with respect to n_e .

ysed discharges. Not only that, the energy confinement time has been also calculated using the neo-Alcator scaling for Ohmically heated tokamak plasma [19] using the equation

$$\tau_E^{\text{NA}} = 0.07 n_{20} a R_0^2 q_a, \quad (2)$$

where n_{20} is electron density in 10^{20} m^{-3} , a is plasma radius in m, R_0 is major radius in m, and q_a is the edge safety factor. The estimated values of τ_E (labelled as τ_E expt) and predicted value of that by neo-Alcator scaling (labelled as τ_E neo-Alc) are plotted in Fig. 4. Both data have been fitted with lines for easy eye guide and error bars have been also given on the seven to eight data. It is seen that both values are almost similar at lower densities and deviate towards the higher densities. These discharges are having high energy confinement times and those values are some-

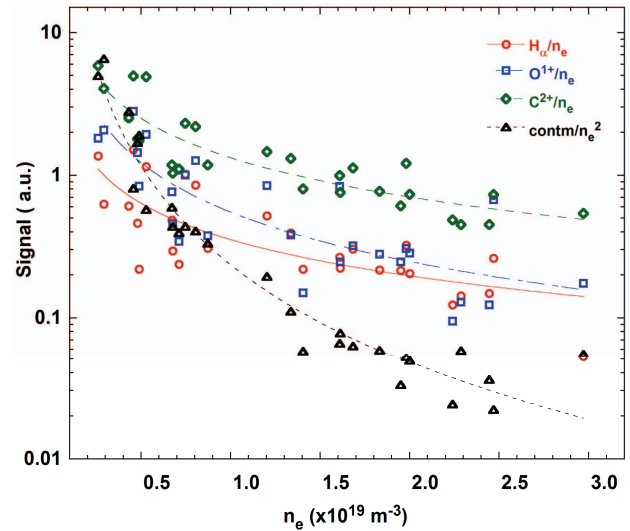


Fig. 5 Signals variation (in a.u.) of H_α and impurities emissions normalized by n_e and visible continuum normalized by n_e^2 plotted with respect to n_e .

times higher than the values predicted by neo-Alcator scaling for Ohmically heated tokamak plasma [12]. Estimated confinement times become even more than 1.5 times of the predicted values. A large number of these discharges lie in the improved Ohmic confinement (IOC) regime, discovered in ASDEX tokamak. In this regime, the linear scaling of $\tau_E \sim n_e$ was extended up to the density limit [8].

The particle and impurity behaviour at the plasma edge of these high performance discharges have been investigated by monitoring H_α , O^{1+} and C^{2+} emission in the visible region as the hydrogen neutral and low ionized impurities ions reside at the plasma edge due to their low ionization energies. These values are 13.6, 35 and 48 eV for hydrogen atom, singly ionized oxygen and doubly ionized carbon, respectively. In these high density and current discharges, it has been found that these spectral lines normalized with n_e , and visible continuum emission normalized with n_e^2 showed a gradual decrease with the increase of electron density as shown in Fig. 5. Although there are scattering in the data, but this does not affect the trend as the variation of n_e normalized intensities are significant. Here also, data have been fitted with lines for easy eye guide. Lower H_α signal at higher n_e points to the reduction of particle recycling and thus improved particle confinement time. Huge drops in O^{1+} and C^{2+} signals clearly indicate the lower edge impurity concentration in these high performance discharges. This is also reflected in the reduction of visible continuum signal measured around 523.4 nm wavelength suggesting lower plasma effective charge, Z_{eff} for the discharges with higher n_e .

Not only that, to understand the core impurity behaviour, the spectral emissions from intermediate and higher ionized stages of several impurities have been monitored using the VUV survey spectroscopic system.

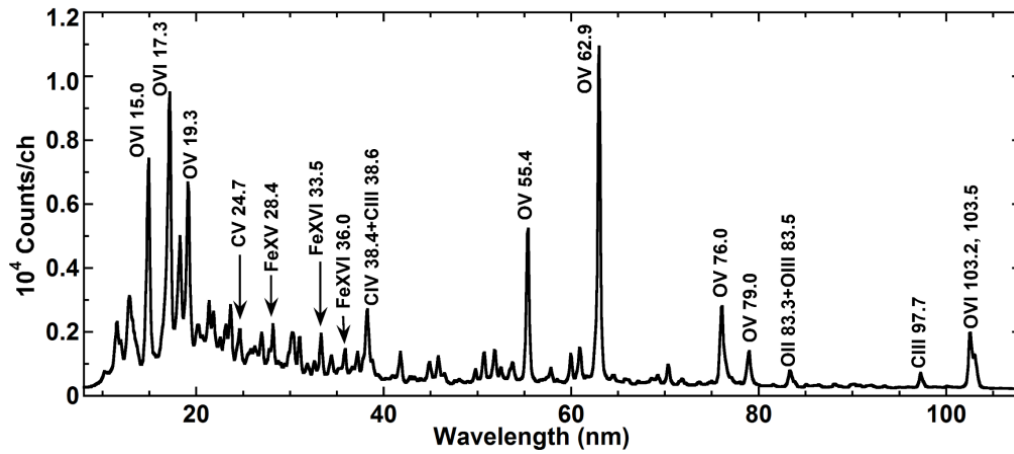
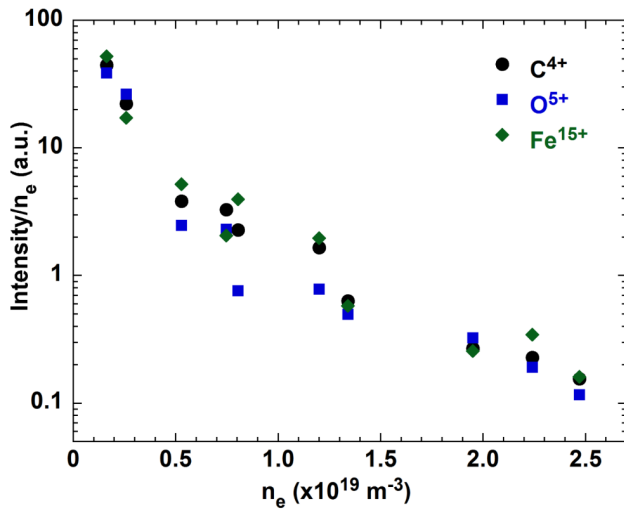
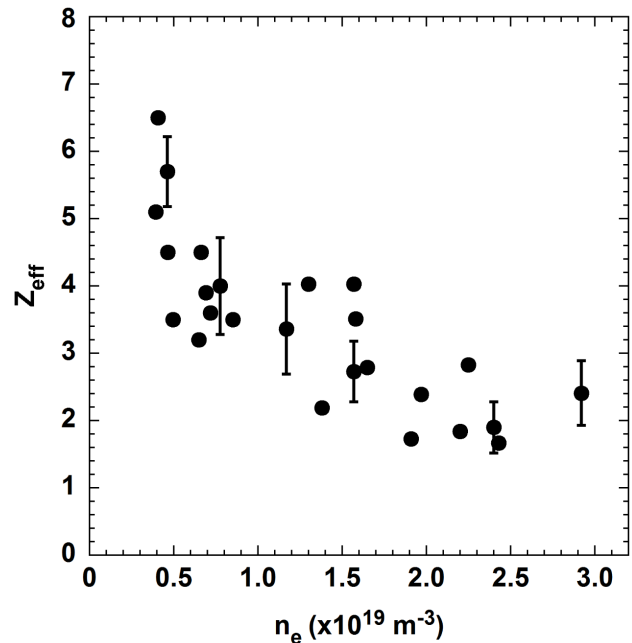


Fig. 6 VUV spectrum from a typical ADITYA plasma.


 Fig. 7 Variation of intensities normalized by n_e (in a.u.) of C^{4+} , O^{5+} and Fe^{15+} impurities emissions plotted with respect to n_e .

The VUV spectrum recorded during the plasma current flat top phase. The spectrometer was operated with 450 grooves/mm grating and CCD integration time was ~ 10 ms. Prominent spectral lines from C^{2+} , C^{3+} , C^{4+} , O^{3+} , O^{4+} , O^{5+} , Fe^{14+} and Fe^{15+} ions are visible in the acquired spectrum as shown in Fig. 6. The analysis of VUV emissions from C^{4+} at 24.7 nm, O^{5+} at 103.2 nm and Fe^{15+} at 33.5 nm have been carried out for several discharges. These emissions mainly coming out from the plasma inner region as the ionization energies of these are quite higher. The ionization energies are 138 eV, 392 eV and 490 eV of the O^{5+} , C^{4+} and Fe^{15+} ions, respectively. As shown in Fig. 7, it is observed that these emissions also decrease very much with increasing n_e as like the emission from plasma edge as depicted in in Fig. 5 Here also line emissions normalized by n_e have been plotted. This implies that along with edge impurity concentration, the core impurity concentration also reduces for the plasmas


 Fig. 8 Variation of Z_{eff} plotted with respect to n_e .

with higher n_e . Indeed, the iron impurity transport study using VUV emissions from Fe ions confirms that the iron concentration reduces with increasing n_e . Here, the absolute intensities of spectral lines at 28.4 nm of Fe^{14+} and at 33.5 nm of Fe^{15+} ions and their ratio have been modelled using impurity transport code, STRAHL [20]. The modelling has been done for the two discharges having lower and higher electron densities. It has been found that intensities and intensity ratios for both the discharges having lower ($0.8 \times 10^{19} \text{ m}^{-3}$) and higher ($1.6 \times 10^{19} \text{ m}^{-3}$) electron densities could be modelled by using the same profile and magnitude of v/D ratio [17]. Here, v is convection velocity and D the diffusion coefficient. The v/D value peaks at ρ , $(r/a) = 0.6$ with a range of -0.28 to -0.42 and reduces towards the core having values in the range of -0.15 to -0.22 at $\rho = 0.1$. However, iron impurity concentration reduced

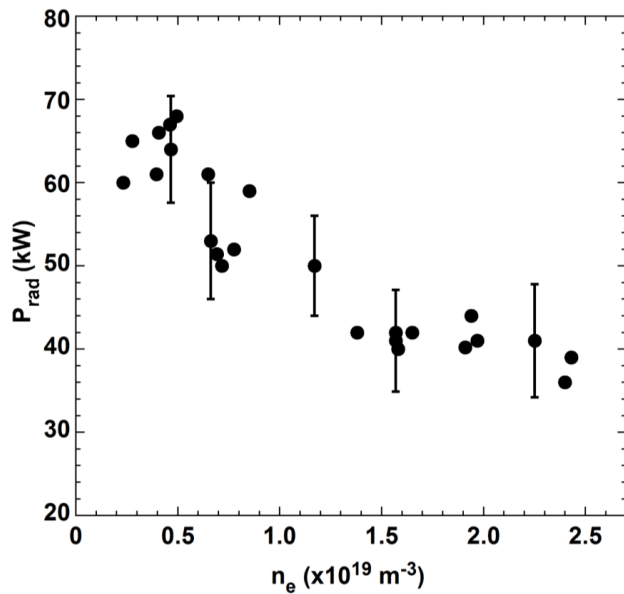


Fig. 9 Variation of radiative power, P_{rad} plotted with respect to n_e .

from 0.1% to 0.07% in the higher density discharge. As indicated from the reduction of C^{2+} and C^{4+} and O^{1+} and O^{5+} emissions and confirmation of decreased iron concentration with increasing electron density, the plasma effective charge, Z_{eff} appears to be lowered with increased n_e . This trend has been observed for the analysed discharges as seen in Fig. 8 in which the variation of Z_{eff} has been plotted with n_e along with error bars on few data. The values of Z_{eff} reduce from ~ 6 to 2 for the plasmas having n_e $0.5 \times 10^{19} \text{ m}^{-3}$ and $2.5 \times 10^{19} \text{ m}^{-3}$, respectively. In addition to that, the reduction of the impurities concentrations are also corroborated by the observed decline in radiative power, P_{rad} as plotted in Fig. 9. The P_{rad} reduces from 65 kW to 38 kW for the discharge with n_e of $2.5 \times 10^{19} \text{ m}^{-3}$. As the radiative power is proportional to the impurity density, the radiation loss becomes less for plasma with lower impurity concentration. These results clearly indicate that the improved confinement for ADITYA plasma is correlated with reduction of impurities concentration and consequently lower radiation loss in those discharges.

4. Summary

The impurity behaviour in the high current and density ADITYA tokamak discharges has been studied by monitoring the visible and VUV emissions from various ionization stages of several impurities. These discharges have been characterised by the higher energy confinement time exceeding than those values predicted by neo-Alcator scaling of energy confinement for Ohmically heated tokamak

plasma. The H_{α} , O^{1+} and C^{2+} emissions in the visible range have been monitored using the optical set-up comprising the optical lens and fiber interference filter and PMT detector. The VUV spectral lines of C^{4+} , O^{5+} and Fe^{15+} ions have been analysed after acquiring those using a VUV survey spectrometer based diagnostic. It has been observed that the impurity emissions from both the plasma edge and core reduces significantly with the increase of plasma electron density, n_e . Not only that, the impurity concentration reduction leads to lower Z_{eff} values for increased n_e discharges. It has been indeed found out through the investigation of iron impurity transport that the impurity concentration reduces in the plasmas with increased n_e . This observation has been also corroborated by measuring the radiation losses from the plasma as it has been seen that radiation loss decreases with increasing plasma n_e . The lower impurity concentration and corresponding lower radiation losses lead to the better ADITYA tokamak plasma properties as reflected in the higher values of energy confinement times for these high current and density discharges.

Acknowledgement

The authors, S. P. and A. K. S. acknowledge the Board of Research in Nuclear Sciences (BRNS), Department of Atomic Energy (DAE) of the Government of India as this work partly supported by the research project grant having sanction No. 39/14/28/2016-BRNS.

- [1] R.C. Isler, Nucl. Fusion **24**, 1599 (1984).
- [2] J. Winter, Plasma Phys. Control. Fusion **38**, 1503 (1996).
- [3] R. Kaita, Plasma Phys. Control. Fusion **61**, 113001 (2019).
- [4] M.B. Chowdhuri *et al.*, Phys. Plasmas **16**, 062502 (2009).
- [5] J. Hong *et al.*, Nucl. Fusion **55**, 063016 (2015).
- [6] L.D. Horton, Plasma Phys. Control. Fusion **42**, A37 (2000).
- [7] A. Komori *et al.*, Nucl. Fusion **49**, 104015 (2009).
- [8] F.X. Soldner *et al.*, Phys. Rev. Lett. **61**, 1105 (1988).
- [9] J.E. Rice *et al.*, Nucl. Fusion **55**, 033014 (2015).
- [10] R. Weynants *et al.*, Nucl. Fusion **39**, 1637 (1999).
- [11] S.B. Bhatt *et al.*, Indian J. Pure Appl. Phys. **27**, 710 (1989).
- [12] R.L. Tanna *et al.*, Nucl. Fusion **57**, 102008 (2017).
- [13] R. Manchanda *et al.*, Nucl. Fusion **62**, 042014 (2022).
- [14] P.K. Atrey *et al.*, IEEE Trans. Plasma Sci. **47**, 1316 (2019).
- [15] K. Tahiliani *et al.*, Plasma Phys. Control. Fusion **51**, 085004 (2009).
- [16] M.B. Chowdhuri *et al.*, Plasma Phys. Control. Fusion **62**, 035015 (2020).
- [17] S. Patel *et al.*, Nucl. Fusion **59**, 086019 (2019).
- [18] M.B. Chowdhuri *et al.*, Plasma Sci. Technol. **15**, 123 (2013).
- [19] R.J. Goldston, Plasma Phys. Control. Fusion **26**, 87 (1984).
- [20] R. Dux, 2004 Impurity transport in tokamak plasmas, IPP-Report, IPP 10/27 (Garching: Max-Planck-Institut fur Plasmaphysik).